JOURNAL OF GEOPHYSICAL RESEARCH, VOL. 115, D11203, doi:10.1029/2009JD012628, 2010

Examination of laboratory-generated coated soot particles: An overview of the LACIS Experiment in November (LExNo) campaign

F. Stratmann,[1] M. Bilde,[2] U. Dusek,[3,4] G. P. Frank,[3,5] T. Hennig,[1,6] S. Henning,[1] A. Kiendler-Scharr,[7] A. Kiselev,[1] A. Kristensson,[2,5] I. Lieberwirth,[8] T. F. Mentel,[7] U. Pöschl,[3] D. Rose,[3] J. Schneider,[9] J. R. Snider,[10] R. Tillmann,[7] S. Walter,[9] and H. Wex[1]

Received 10 June 2009; revised 17 September 2009; accepted 14 December 2009; published 4 June 2010.

[1] In the suite of laboratory measurements described here and in companion articles we deal with the hygroscopic growth and activation behavior of coated soot particles synthesized to mimic those of an atmospheric aerosol originating from biomass combustion. The investigations were performed during the measurement campaign LACIS Experiment in November (LExNo) which took place at the Leipzig Aerosol Cloud Interaction Simulator (LACIS). The specific goals of this campaign were (1) to perform a critical supersaturation measurement intercomparison using data sets from three different cloud condensation nucleus (CCN) instruments (two static thermal gradient type, one stream-wise thermal gradient type) and LACIS, (2) to examine particle hygroscopic growth (hydrated particle size as function of relative humidity) for particle characteristics such as aerosol mass spectrometer (AMS) measured soluble mass and particle morphology, and (3) to relate critical supersaturations derived from both measurements of soluble mass and high-humidity tandem differential mobility analyzer (HH-TDMA) determined growth factors to critical supersaturations measured by means of the CCN instruments. This paper provides information on the particle synthesis techniques used during LExNo, an overview concerning the particle characterization measurements performed, and, by proving relations between measured composition, hygroscopic growth, and activation data, lay the foundations for the detailed investigations described in the companion studies. In the context of the present paper, excellent agreement of the critical supersaturations measured with three different CCN instruments and LACIS was observed. Furthermore, clear relations between coating masses determined with AMS and both hygroscopic growth factors at 98% RH and measured critical supersaturations could be seen. Also, a strong correlation between measured hygroscopic growth (growth factors at 98%) and measured critical supersaturation for all of the differently coated soot particles (coating substances being levoglucosan and/or ammonium (hydrogen) sulfate) was found. This is clearly indicative of the possibility of predicting the critical supersaturation of coated soot particles based on hygroscopic growth measurements using Köhler theory.

Citation: Stratmann, F., et al. (2010), Examination of laboratory-generated coated soot particles: An overview of the LACIS Experiment in November (LExNo) campaign, *J. Geophys. Res.*, *115*, D11203, doi:10.1029/2009JD012628.

1. Introduction

[2] Atmospheric aerosols play an important role in the Earth system. They scatter and absorb radiation and induce the formation of clouds and precipitation. The radiative

[1]Institute for Tropospheric Research, Department of Physics, Leipzig, Germany.
[2]Department of Chemistry, University of Copenhagen, Copenhagen, Denmark.
[3]Biogeochemistry Department, Max Planck Institute for Chemistry, Mainz, Germany.
[4]Now at Institute for Marine and Atmospheric Research, Utrecht University, Utrecht, Netherlands.
[5]Now at Department of Physics, Lund University, Lund, Sweden.
[6]Now at Institute for Applied Environmental Science, Stockholm University, Stockholm, Sweden.
[7]ICG-II: Troposphere, Research Centre Juelich, Juelich, Germany.
[8]Max Planck Institute for Polymer Research, Mainz, Germany.
[9]Particle Chemistry Department, Max Planck Institute for Chemistry, Mainz, Germany.
[10]Department of Atmospheric Science, University of Wyoming, Laramie, Wyoming, USA.

0148-0227/10/2009JD012628

effects of aerosols can be strongly influenced by water vapor uptake and hygroscopic growth of the particles under subsaturated conditions (relative humidity, RH, < 100%). Furthermore, at water vapor supersaturation (RH > 100%), aerosol particles can be activated as cloud condensation nuclei (CCN). Both the optical properties and the ability of atmospheric aerosol particles to act as CCN depend on their size and chemical composition [*Forster et al.*, 2007].

[3] An important constituent of the atmospheric aerosol is particles from fossil fuel and biomass combustion, which consist of soot (black/elemental carbon) and a wide range of organic and inorganic substances including levoglucosan, ammonium sulfate, and ammonium hydrogen sulfate. Levoglucosan is a characteristic marker and major component of biomass burning aerosols with mass concentrations of up to 7 $\mu g/m^3$ and mass fractions of up to 5% [e.g., *Andreae and Merlet*, 2001; *Reid et al.*, 2005a, 2005b; *Simoneit et al.*, 1999; *Kawamoto et al.*, 2003; *Zdrahal et al.*, 2002; *Simpson et al.*, 2004; *Graham et al.*, 2002]. Moreover, it is a hygroscopic substance and promotes water uptake by aerosol particles [*Mochida and Kawamura,* 2004]. In the atmosphere, combustion aerosols can undergo chemical aging and cloud processing, during which secondary chemical components are formed or condense on the particles and enhance their hygroscopicity and CCN activity. Among the most abundant and most hygroscopic secondary chemical components of atmospheric aerosols are ammonium sulfate and ammonium hydrogen sulfate, which are formed by gas-phase and multiphase oxidation of sulfur dioxide and other sulfur-containing trace gases and subsequent neutralization with ammonia [*Seinfeld and Pandis*, 1998].

[4] There are a large number of studies that examine the ability of atmospheric aerosol particles to act as CCN. Among them are so-called CCN closure studies, in which the measured particles' ability to act as CCN is compared to this ability derived from either measured hygroscopic growth or from information concerning the chemical composition of the particles. Closure studies in general help to increase the understanding of the underlying processes. *Broekhuizen et al.* [2006], *Stroud et al.* [2007], and *Medina et al.* [2007] all give overviews on CCN closure studies for atmospheric aerosol particles. In summary, those studies that were able to achieve closure were generally not influenced by strong anthropogenic sources and had low concentrations of organic carbon in the aerosol phase [*Broekhuizen et al.*, 2006]. For studies that did not achieve closure, CCN concentrations were generally overpredicted, and the discrepancy has generally been attributed to an incomplete understanding of the aerosol composition, especially the role of organic species [*Stroud et al.*, 2007].

[5] An advantage of laboratory studies is that the generated particles can be tailored to the subjects one wants to examine. Therefore, also, a large number of laboratory based studies on hygroscopic growth and activation of particles of different chemical composition has been performed in the last years, often examining different organic compounds (for an overview on a variety of these studies, see *Wex et al.* [2008]). While it has been described that small amounts of inorganic salts can strongly influence the particle activation behavior of particles consisting of slightly soluble substances [*Bilde and Svenningsson*, 2004], laboratory studies examining the hygroscopic properties of uncoated or coated soot particles, i.e., particles consisting of an insoluble and a soluble part, are, to our knowledge, still lacking until today.

[6] In the suite of laboratory measurements described here, and in companion articles [*Henning et al.*, 2010, *Kiselev et al.*, 2010; *Snider et al.*, 2010], we analyze the properties of particles synthesized to mimic those of an atmospheric aerosol originating from biomass combustion. Specifically, we examine internal aerosol mixtures of water insoluble inorganic carbon (soot), ammonium (hydrogen) sulfate and levoglucosan. Our intent is to shed light on the importance of chemical composition and particle morphology for subsaturated and supersaturated particle growth. The study took place at the Leipzig Aerosol Cloud Interaction Simulator (LACIS), a laboratory designed to examine particle hygroscopic growth in the subsaturated regime, condensation nucleation and growth in the supersaturated regime [*Stratmann et al.*, 2004; *Wex et al.*, 2005, 2006]. LACIS became an ACCENT (Atmospheric Composition Change the European Network of Excellence) infrastructure site in 2005, and its first measurement campaign, called LExNo (LACIS Experiment in November), is summarized here.

[7] The specific goals of this campaign were (1) to perform a critical supersaturation measurement intercomparison using data sets from three different CCN (Cloud Condensation Nucleus) instruments (two static thermal gradient type, one stream-wise thermal gradient type) and LACIS, (2) to examine particle hygroscopic growth (hydrated particle size as function of relative humidity) for particle characteristics such as aerosol mass spectrometer (AMS) measured soluble mass, and particle morphology, and (3) to relate critical supersaturations derived from both, measurements of soluble mass, and high-humidity tandem differential mobility analyzer (HH-TDMA) determined growth factors, to critical supersaturations measured by means of the CCN instruments. Investigations concerning particles morphology comprise measurements of mobility-equivalent and aerodynamic-equivalent particle diameters and examination of electron micrographs.

[8] This paper provides detailed information on the particle synthesis techniques used during LExNo, an overview concerning the particle characterization measurements performed, and an introduction to the results of the companion studies. For further details on the different topics, the reader is referred to *Henning et al.* [2010] (subsaturated growth and connections between critical supersaturation and particle properties), *Kiselev et al.* [2010] (particle shape and density characterizations) and *Snider et al.* [2010] (CCN instruments intercomparisons).

2. Experiment

[9] The measurement campaign LExNo (LACIS Experiment in November) took place at the ACCENT infrastructure site LACIS (Leipzig Aerosol Cloud Interaction Simulator) from 14 November to 2 December 2005. Coated soot particles were generated in the laboratory in order to mimic an aged biomass combustion aerosol. The particles were characterized with respect to composition and morphology. Varying these properties, hygroscopic growth and critical supersaturation needed for activation were determined.

[10] Composition and mass concentrations of the nonrefractory particle components (i.e., mainly the coating) was

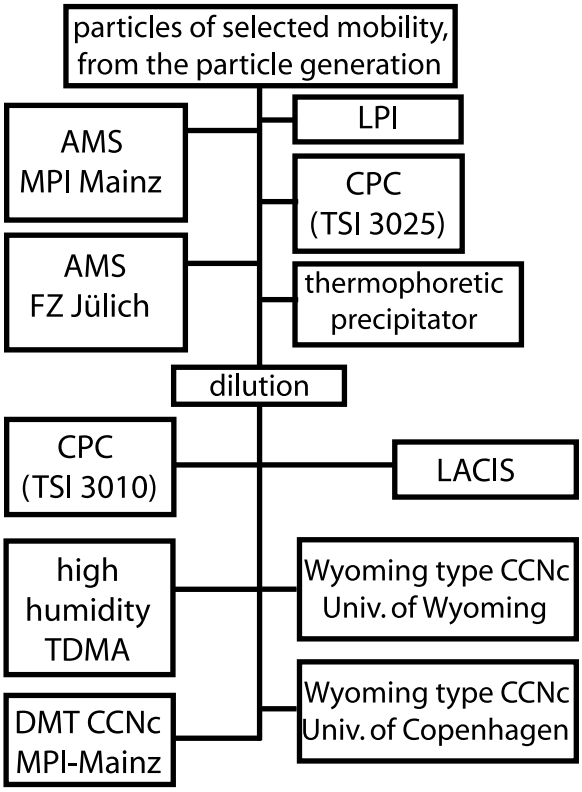

Figure 1. Setup of instruments used in LExNo.

measured utilizing two Quadrupole Aerosol Mass Spectrometers (AMS) [*Jayne et al.*, 2000]. The AMSs were provided and operated by the Max Planck Institute for Chemistry, Mainz, Germany, and the Research Centre Jülich, Jülich, Germany. For structural analysis, vacuum aerodynamic diameters of the investigated particles were determined with the two AMSs and a single-stage Low Pressure Impactor (LPI), as described by *Fernández de la Mora et al.* [1990]. Transmission Electron Microscope (TEM) grids were sampled with a thermophoretic precipitator [*Messerer et al.*, 2003] and analyzed at the Max Planck Institute for Polymer Research, Mainz, Germany.

[11] Hygroscopic growth factors up to relative humidities of 98% were determined by means of a HH-TDMA [*Hennig et al.*, 2005]. Critical supersaturations were measured with three different CCN instruments, and with LACIS. This redundancy is necessary since instrument-dependent bias due to the difficulty of determining the maximum supersaturation reached in the instruments, [*Snider et al.*, 2006; *Lance et al.*, 2006] is a vexing issue in CCN measurement. In detail, two Wyoming type CCN instruments [*Snider et al.*, 2003] were provided and operated by the University of Wyoming and by the University of Copenhagen. Also, a continuous flow stream-wise thermal gradient CCN counter (DMT (Droplet Measurement Techniques) [*Roberts and Nenes*, 2005]) was operated by the Max Planck Institute for Chemistry, Mainz, [*Rose et al.*, 2008], and LACIS was run as a CCN instrument as described by *Wex et al.* [2006].

[12] The number concentrations of the investigated particles were measured with two Condensation Particle Counters (CPCs), i.e., a TSI 3025 parallel to the two AMS, a TSI 3010 and another TSI 3025, parallel to the HH-TDMA and the CCN instruments. A schematic diagram of the experimental setup is shown in Figure 1. Because of the low instrumental sensitivities, the AMS, the LPI, and the thermophoretic precipitator were fed from the generator directly without any dilution. Typical number concentrations delivered to the AMSs, were between 5000 and 10000 cm^{-3}. To provide the sample volume flow needed and the number concentrations suitable for the HH-TDMA and the CCN instruments, the aerosol was diluted by means of a modified PALAS VKL-10 dilution system running at a dilution ratio of about 1/10.

3. Particle Generation

[13] The particles investigated in the framework of this study were composed of soot, levoglucosan, and ammonium (hydrogen) sulfate. The experimental system shown in Figure 2 was applied to produce the particles. To facilitate the investigation regarding the importance of particle morphology on hygroscopicity and cloud droplet activation, two types of soot particles were generated: compacted and noncompacted particles. In both cases, soot particles were first produced by means of a spark generator (Palas, GFG 1000). Compaction of these particles was achieved by passing them over a pool of liquid 2-propanol [*Kütz*, 1994] contained in the bottom of a horizontal glass conditioning tube. Adsorption of the propanol vapor onto the loose agglomerates causes them to collapse into a more compact shape. If no compaction was desired, the particles were passed through an identical empty conditioning tube without liquid. To remove the propanol vapor from the carrier gas and also the propanol bound to the particles, the aerosol was fed through an annular diffusion dryer filled with activated charcoal. However, as described below, not all of the propanol was removed by the dryer. For consistency, the noncompacted dry soot particles were passed through the diffusion dryer as well. Downstream of the dryer, the aerosol was fed through a Vienna-type Differential Mobility Analyzer (DMA1) [*Winklmayr et al.*, 1991] which was operated at a fixed mobility diameter of 100 nm. Behind the DMA, the mobility selected soot particles (noncompacted and compacted) were coated. Inside two coating furnaces, the aerosol was passed over heated reservoirs of (1) ammonium sulfate (temperature between 93°C and 170°C) and (2) levoglucosan (temperature between 80°C and

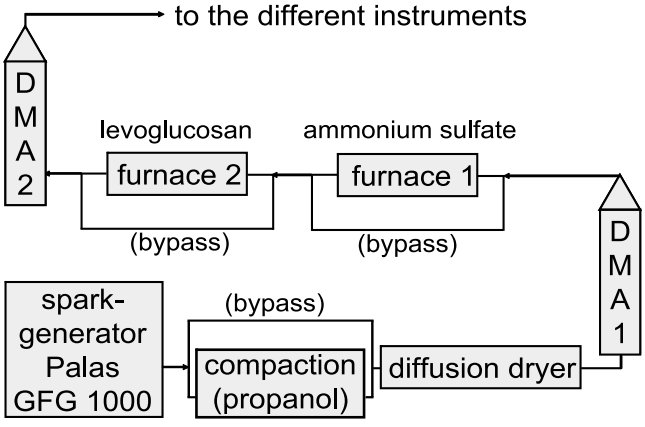

Figure 2. Setup of particle generation and coating devices.

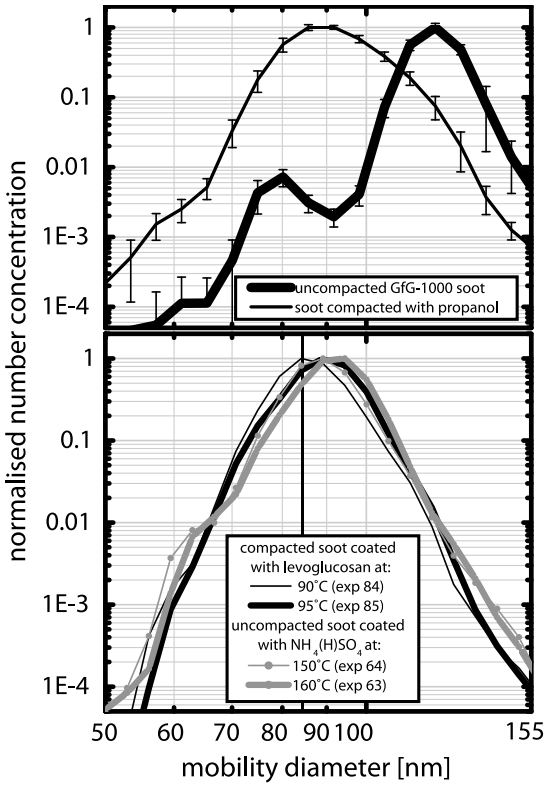

Figure 3. (top) Normalized average measured particle size distributions of pure soot, as generated by the GFG 1000 (thick line), and the corresponding size distribution obtained when soot particles were subsequently compacted with propanol (thin line). (bottom) Normalized particle size distributions as resulting from different coating processes for particles that were initially 100 nm (selected with DMA1).

106°C). Regarding ammonium sulfate, the higher temperatures in the furnaces were such that thermal decomposition could have occurred [*Kiyoura and Urano*, 1970; *Halstead*, 1970]. Analysis of the AMS data concerning ammonium sulfate coated soot particles revealed a molar ratio of NH_4 to SO_4 of 1.1 with an overall uncertainty of about 10%. This suggests that the main coating component was ammonium hydrogen sulfate (NH_4HSO_4). Since a certain amount of ammonium sulfate may be present in the coating, from now on the expression ammonium (hydrogen) sulfate will be used. Decomposition was not expected for levoglucosan as it only starts to decompose above 110°C [*Oja and Suuberg*, 1999]. As can be seen in Figure 2, possible options for the generation of particle coatings were: no coating, coating with either ammonium (hydrogen) sulfate or levoglucosan, or coating with both ammonium (hydrogen) sulfate and levoglucosan. In this context it should be noted that here coating stands for condensing material on the soot particles' complex surfaces. This, due to the complex morphology of the soot particles, does not necessarily imply generation of well-defined layers.

[14] Downstream of the coating furnaces, the particles were passed through a second DMA (DMA2) where the mobility-equivalent diameter of the particles was set. As discussed below, the focus was on relatively thin coatings (less than approximately 20 nm) and the soot particles collapsed during the coating process. Therefore, the mobility-equivalent diameter selected by DMA2 was set to 84 nm (close to the maximum of the size distribution of the coated particles; see Figure 3, bottom), unless stated otherwise.

[15] The different test aerosols that were synthesized and sampled during LExNo are summarized in Tables 1a and 1b. Each experiment is assigned a number which is used here and in the companion papers to stratify the LExNo data set.

[16] Figure 3 shows representative particle number size distributions (size spectra), normalized to 1 at their peak amplitude. Figure 3 (top) depicts average measured particle size distributions of pure soot, as generated by the GFG 1000 (thick line), and the size distribution for soot particles compacted with propanol (thin line). The collapse of the particles due to the compaction can clearly be seen by the shift of the main maximum. Figure 3 (bottom) depicts particle size distributions resulting from different coating processes for particles that were initially 100 nm (selected with the first DMA). The examples shown are distributions for soot particles that had not been compacted with propanol and were coated with ammonium (hydrogen) sulfate (at a furnace temperature of 150°C and of 160°C), and soot particles that were compacted and subsequently coated with levoglucosan (at 90°C and at 95°C). The vertical line indicates the 84 nm diameter at which particles were selected with DMA2 prior to provision to the different instruments. In these examples and in general, higher furnace temperatures led to thicker coatings. A comparison of the top and bottom plots of Figure 3 demonstrates clearly that a coating with ammonium (hydrogen) sulfate alone, without a prior compaction of the soot particles, led to a collapse comparable to that caused by the treatment with propanol vapor. Throughout LExNo, soot particles generated with the spark generator were found to collapse easily by condensation of either propanol, levoglucosan or ammonium (hydrogen) sulfate vapors.

[17] To get a visual impression of the generated particles and to obtain information about the particle morphology and primary particle size via image analysis, downstream of the second DMA, particles were sampled for TEM (Transmission Electron Microscope) analysis with a thermophoretic precipitator [see *Messerer et al.*, 2003]. Figure 4 depicts various types of particles as produced by the generator described above. Figure 4a shows the particle morphology (loose soot agglomerate) sampled at the exit of DMA1. In accordance with the findings shown in Figure 3, the exposure of these agglomerates to propanol vapor (with subsequent removal of the propanol) leads to a collapse, i.e., compaction of the aggregates (Figure 4b). Figures 4c and 4d depict originally noncompacted soot particles coated with ammonium (hydrogen) sulfate and levoglucosan, respectively. Similar to what was inferred from the size distributions (Figure 3), coating with ammonium (hydrogen) sulfate and levoglucosan also leads to compaction

Table 1a. Experiments With Particles of Pure Ammonium Sulfate and Pure Levoglucosan Generated From an Atomizer and Fed to the Different Instruments for Calibration Purposes

	Experiment Number								
	42	43	44	45	46	54	55	56	57
Pure ammonium sulfate	x	x	x	x	x				
Pure levoglucosan						x	x	x	x

Table 1b. Different Temperatures That Were Set at the Furnaces for the Different Experiments With Coated Soot Particles

Experiment Number	Compaction of Soot in Propanol Conditioner	Temperature in Furnace 1 With Ammonium Sulfate (°C)	Temperature in Furnace 2 With Levoglucosan (°C)
48			102
49			100
50			104
51			102
52			104
60			104
61			106
62		170	
63		160	
64		150	
73		140	
74	x	140	
75	x	130	
80	x	100	
81		100	
82	x	93	
84	x		90
85	x		95
86	x		92.5
88	x	109	95
91	x	115	91
92	x	115	80

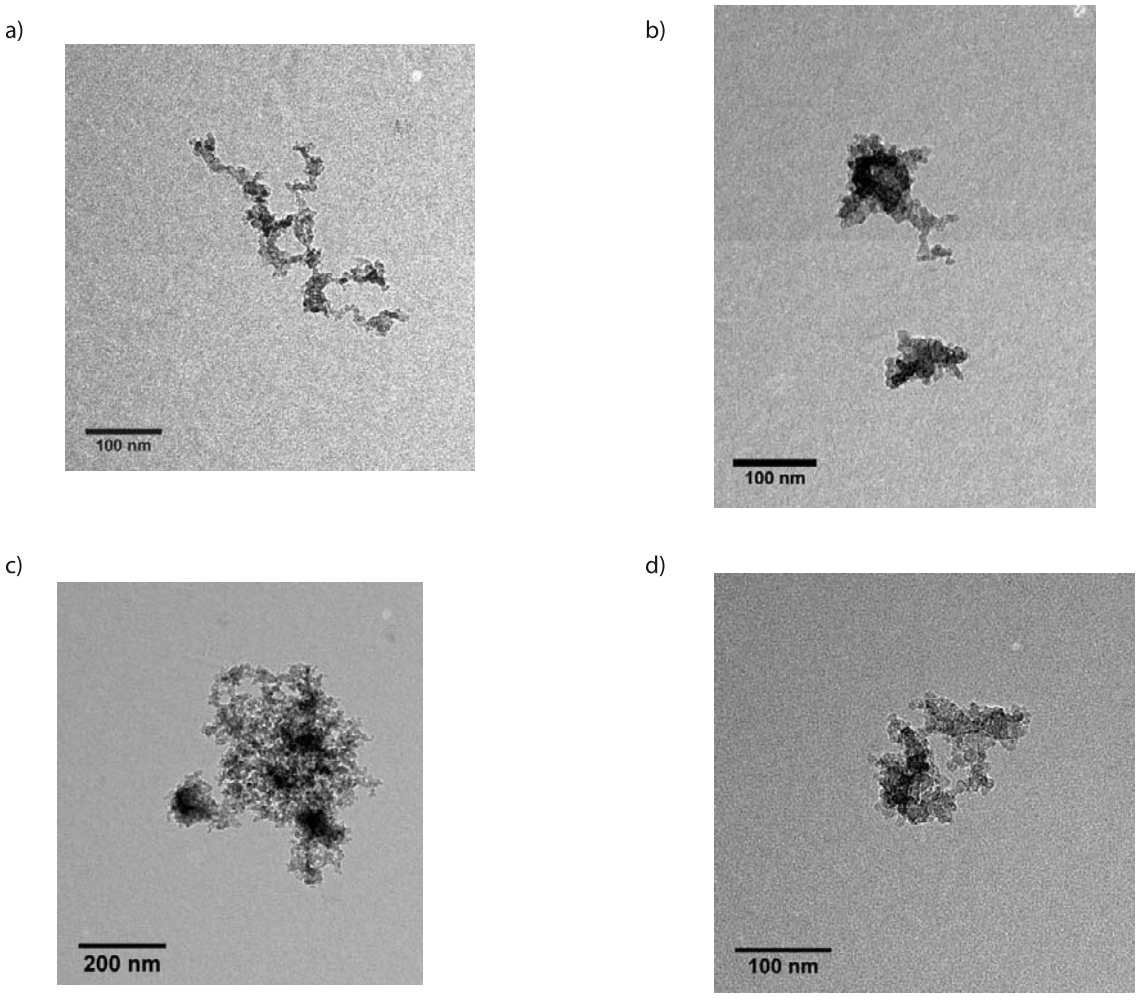

Figure 4. TEM pictures of generated particles: (a) uncompacted soot particles, (b) compacted soot particles, (c) uncompacted soot coated with ammonium (hydrogen) sulfate, and (d) uncompacted soot coated with levoglucosan.

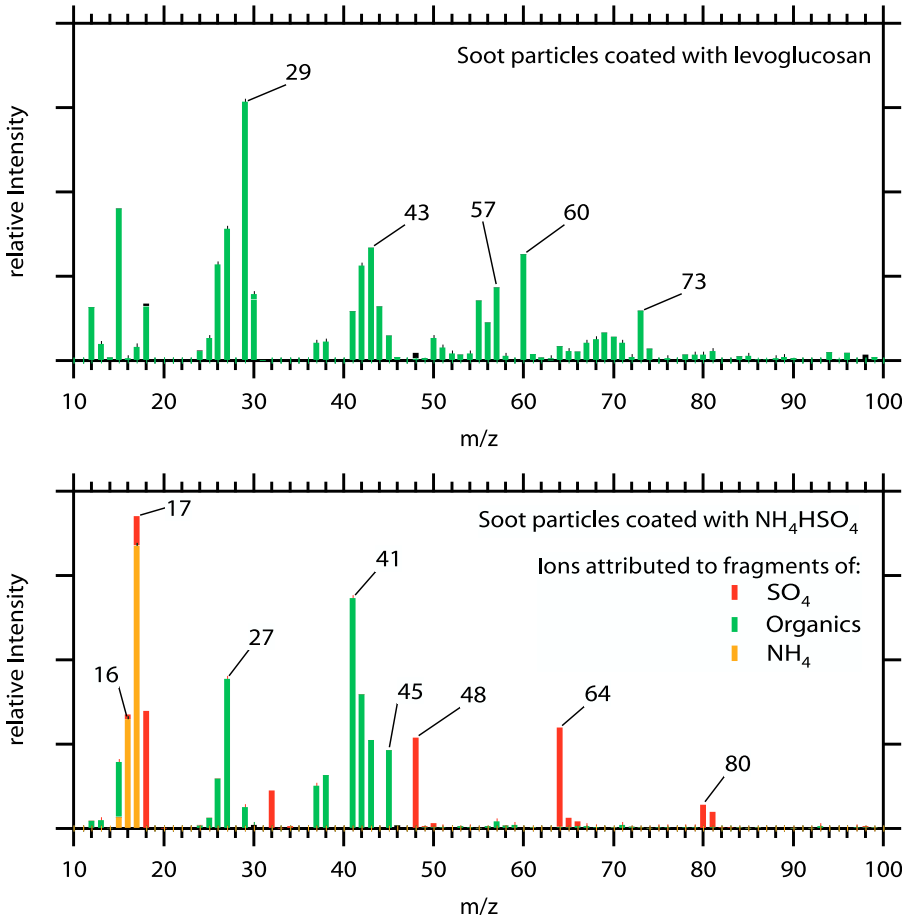

Figure 5. AMS mass spectra of soot particles coated with (top) levoglucosan and (bottom) NH_4HSO_4. The organic signatures denoted in green in the bottom plot are likely due to propanol that was used during the experiment to compact the soot particles.

of the soot particles, with the effect being more pronounced for ammonium (hydrogen) sulfate as to be seen from Figure 4.

[18] For particles with morphology typical of that shown in Figures 4a–4d, a DMA is not well-suited for determining the quantity of condensed material. For this purpose we used two AMSs. The two AMSs were simultaneously calibrated with ammonium nitrate particles and polystyrol latex spheres from the same particle generators. With this calibration the concentrations of sulfate and organics measured by the two instruments during LExNo agreed within 7% (sulfate) and 4% (organics), in a concentration range between 0.2 and 9 μg m^{-3}. After this satisfying agreement of the two instruments the data were merged to one data set for further analysis. Figure 5 shows typical AMS mass spectra of coated soot particles as observed during LExNo. When levoglucosan was used as the coating material (Figure 5, top), the measured mass spectrum is almost identical to the mass spectra obtained from laboratory measurements of pure levoglucosan by *Schneider et al.* [2006] and *Alfarra et al.* [2007], with typical ion signatures at m/z 29, 43, 44, 57, 60, 73. Therefore the signals observed are interpreted as a levoglucosan coating on the surface of the particles.

[19] When ammonium sulfate was used, the coatings of the soot particles were found to consist of ammonium, sulfate, and an additional substance that was most likely of organic nature (Figure 5, bottom). The organic ions 27, 41, and especially 45 (presumably $C_2H_4OH^+$) suggest that this organic compound is of alcoholic nature; thus propanol appears to be the most likely candidate. It should be noted that for coating with levoglucosan, no significant signatures of propanol were found in the particles. The presence of ammonia ions (m/z 16 and 17), sulfate ions (m/z 48, 64, 80, 81) and other fragments (m/z 18 and 32) [*Allan et al.*, 2004], together with the observed molar ratio of NH_4 to SO_4 of 1.1, suggests that the coating furnace is useful for the generation of ammonium (hydrogen) sulfate coatings. The presence of propanol in the ammonium (hydrogen) sulfate coatings, although the particles were heated to temperatures of at least 90°C while being coated, together with no propanol being identified in the levoglocusan coated particles, could be indicative for interactions between the propanol, the ammonium (hydrogen) sulfate, and the soot core during the coating process. In this study, the propanol will be treated as an additional soluble organic substance.

[20] As the main focus of this paper is to describe the LExNo experiment itself and the applied techniques, in the following, only a brief summary and outlook concerning the results obtained during LExNo will be given. First, results regarding the measurement of aerodynamic particle sizes using an LPI and two AMS instruments will be presented.

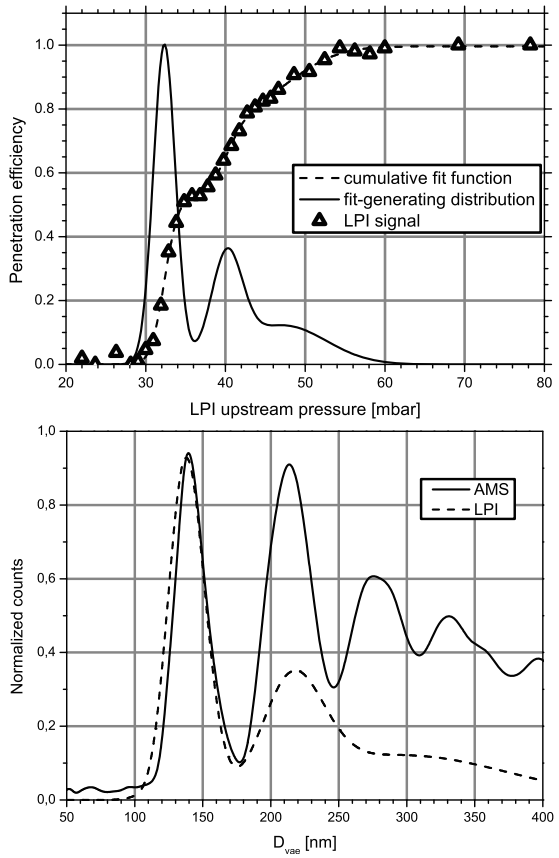

Figure 6. (top) Measured LPI signal and derived particle size distribution and (bottom) normalized count distributions as derived from the LPI (charge counts) and from the AMS (mass counts) measurements as function of D_{vae} for pure levoglucosan particles with a mobility diameter of 95 nm.

Then, critical supersaturations as measured with 3 different CCN instruments and LACIS will be compared and the relations between the mass of coating and particle hygroscopic growth and activation, will be summarized. Finally, the relation between particle hygroscopic growth and activation behavior will be presented and discussed.

4. Measurement of Aerodynamic Particle Sizes Using LPI and AMS

[21] Electrical mobility size selection does not provide unambiguous characterization of coated soot particles. Additional data on the internal structure of coated soot agglomerates can be obtained from the measurements of the aerodynamic diameter, which is sensitive to the porosity and shape of the particles. During LExNo the vacuum aerodynamic diameter, or the aerodynamic diameter in the free-molecular regime (D_{vae} [see, e.g., *Van Gulijk et al.*, 2004; *Schneider et al.*, 2006]) was determined with an LPI and the two AMS instruments. Figure 6 (top) shows an LPI measured penetration efficiency curve (fraction of particles that transmit their charge via the impactor to an electrometer) for pure levoglucosan particles with a mobility diameter of 95 nm as function of LPI upstream pressure. In addition, the result of fitting the superposition of three error functions to the impaction efficiency curve is given. Also shown is the sum of the fit-generating Gauss distributions versus LPI upstream pressure. Since the pressure in the upstream chamber of the LPI is the only variable controlling the critical Stokes number of a particle of any given aerodynamic size and thus, its impaction probability, it can be uniquely converted into the vacuum aerodynamic diameter D_{vae} of the transmitted particles. For that, the LPI was calibrated with the mobility-selected near-spherical particles of known density (ammonium sulfate). With this calibration, the resulting Gauss distributions can be interpreted as number (aerodynamic) size distributions. These normalized number distributions are compared to the mass distributions measured with the AMS. In Figure 6 (bottom), normalized count distributions, as derived from the LPI (charge counts) and from the AMS (mass counts) measurements, are plotted as function of D_{vae}, which is directly obtained from the AMS data set. Considering the modal values (positions of maxima) of the plotted distributions, singly and doubly charged particles can easily be identified, with the two different methods showing the occurrence of the respective particles at the same vacuum aerodynamic diameters. Note that the fraction of multiple charged particles in the AMS distributions seems to be significantly higher compared to that of the LPI data. This is the result of the different measuring principles utilized in the two instruments: the signal detected in LPI is proportional to the number of charges delivered by particles and thus to the number of particles, whereas the signal of AMS is proportional to particle mass.

[22] Figure 7 summarizes the aerodynamic particle size measurements carried out during LExNo by comparing modal vacuum aerodynamic diameters D_{vae} as derived from LPI and AMS measurements for different kinds of particles (see caption of Figure 7). The aerodynamic diameters determined with the two different methods are in good agreement for all different kinds of particles investigated, as indicated by the slope of 1.037 and R^2 of 0.908 of the linear fit given in Figure 7. The sensitivity of both instruments to changes in effective density due to the coating of the soot particles suggests that LPI or AMS measurements of D_{vae} of mobility-selected nonspherical particles can be used to quantify the mass of the coating material, a property that normally is derived from the AMS mass spectra.. The detailed formulation

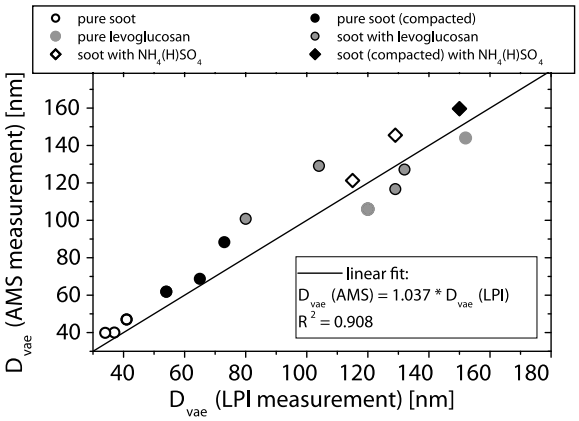

Figure 7. Comparison of vacuum aerodynamic diameter (D_{vae}) as derived from LPI and from AMS measurements.

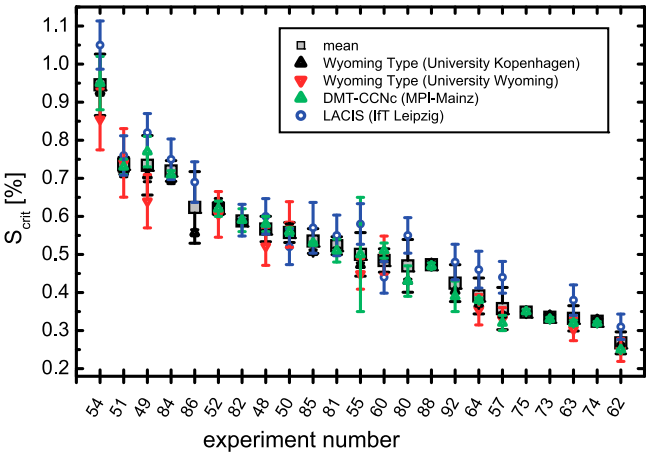

Figure 8. Critical supersaturations measured with the three different CCN instruments and LACIS, and the mean values, for the different coated particles produced during LExNo.

of this method and the comparison to the AMS data are given by *Kiselev et al.* [2010].

5. Comparison of Critical Supersaturations as Measured With Three CCN Instruments and LACIS

[23] The critical supersaturations measured by the three CCN instruments and with LACIS were compared for all experiments performed during LExNo. Figure 8 summarizes the measured critical supersaturations as a function of experiment number, i.e., for all different types of particles and experimental conditions considered. Given are the critical supersaturations as measured with the three different CCN instruments (and their respective uncertainties [see *Snider et al.*, 2010]) and with LACIS, and the mean and standard deviation of these four values. Figure 8 was arranged such, that the mean critical supersaturation decreases along the *x* axis. The test particle type can be found by cross referencing the experiment number (*x* axis) with Tables 1a and 1b. This arrangement of the data was chosen to ease the view on the agreement of the results from the different instruments.

[24] It can be seen, that all of the critical supersaturations are in agreement within the mean value ±1 standard deviation, i.e., within the measurement uncertainties. There is a slight systematic shift of the values obtained with LACIS; that is, those critical supersaturations are slightly larger than the mean value, exceeding the mean by about 0.04% (absolute) on average. However, this shift is still within the measurement uncertainty.

[25] The reason for this small discrepancy is not yet clear. But it is interesting to note that the technique used for evaluating the critical supersaturation is different for LACIS, compared to that employed by the three CCN instruments. From these instruments, the activated fraction of the particles is derived, and the critical supersaturation is taken to be the supersaturation corresponding to 50% of the particles activating. In contrast, the measurement made by LACIS is the mode size of the nascent cloud droplets. This size increases drastically once the particles activate, and this increase is used to derive the critical supersaturation [*Wex et al.*, 2006]. It should be noted that all of the CCN instruments and LACIS were calibrated with ammonium sulfate particles both at the investigator's home laboratories and at the IfT laboratory immediately prior to LExNo.

[26] A detailed study of the LExNo CCN instrument intercomparison is described by *Snider et al.* [2010].

6. Relation Between Mass of Coating and Hygroscopic Growth

[27] Figure 9 shows the equilibrium diameters measured with the HH-TDMA at 98% RH in comparison to the average mass of coating material per particle. This quantity was calculated from the nonrefractory mass concentration measured by the AMS in the integrating mode (not size resolved), divided by the number concentration of particles entering the AMS as measured by the CPC. Multiple charged particles were neglected, because the size distribution in Figure 3 (bottom) indicates that the relative abundance of particles with 125 nm (corresponding to a double-charged 84 nm particle) was only about 1%. Error bars result from the AMS inherent uncertainties (*x* direction) and the achieved accuracy in adjusting the relative humidity (*y* direction).

[28] All experiments shown in Figure 9 were performed for the same dry mobility diameter, i.e., 84 nm, at the second DMA. Experiments with soot particles which were compacted by propanol vapor could not be distinguished from those with noncompacted particles, as both data sets exhibit similar behavior. This is due to the fact that coating with levoglucosan or ammonium (hydrogen) sulfate led to collapsing of the soot particles (see Figure 4), and no truly noncompacted soot particles were investigated.

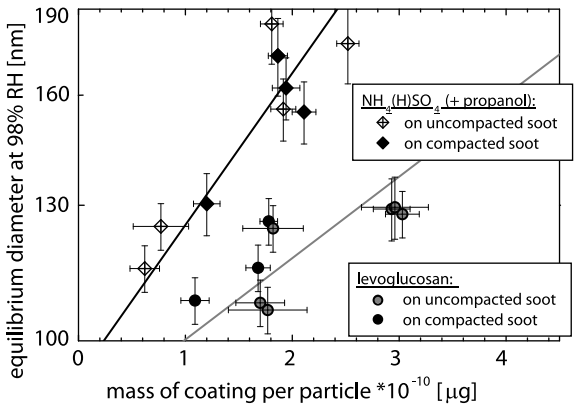

Figure 9. Equilibrium diameters measured with the HH-TDMA at 98% RH for the different experiments shown in comparison to the mass of coating per particle as measured with the AMS. The dry diameter of the particles was 84 nm in all cases. For the experiments during which the coating consisted of ammonium (hydrogen) sulfate, the mass of ammonium and sulfate together with the mass of the additionally detected organic compound was used.

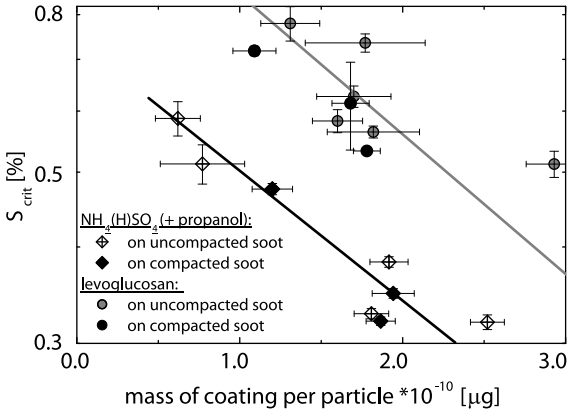

Figure 10. Critical supersaturations for activation measured with the DMT-CCN counter for the different experiments shown in comparison to the mass of coating per particle as measured with the AMS. The symbols are the same as those used in Figure 9, and dry particle diameter was 84 nm in all cases.

[29] For the experiments for which ammonium (hydrogen) sulfate was the coating substance, an additional organic substance (most likely propanol) was detected as mentioned previously. The mass ratio of ammonium (hydrogen) sulfate to the organic substance in the coatings was comparable in all the experiments, being 1.03 ± 0.1. Therefore, in the case of coating with ammonium (hydrogen) sulfate, Figure 9 shows the sum of the masses of ammonium, sulfate and this additional organic substance (from now on assumed to be propanol). For both coatings, i.e., ammonium (hydrogen) sulfate (+propanol) and levoglucosan, a correlation between the hygroscopic growth and the mass of the coating can be seen; that is, hygroscopic growth increases with increasing mass of the coating. Correlation between the detected mass of coating and the observed hygroscopic growth is smaller for levoglucosan coatings with a R^2 value of 0.59, while R^2 is 0.8 in the case of the ammonium (hydrogen) sulfate (+propanol) coating. For similar coating masses, levoglucosan coatings feature smaller hygroscopic growth factors than ammonium (hydrogen) sulfate (+propanol) coatings, thus indicating lower hygroscopicity of levoglucosan compared to that of the ammonium (hydrogen) sulfate (+propanol) coating, as to be expected.

7. Relation Between Mass of Coating and Critical Supersaturation

[30] Figure 10 shows the measured critical supersaturations in connection with the mass of coating per particle as determined by the AMS instruments. Due to the fact that the DMT-CCN counter had the most complete data set, values from this instrument were used in the comparison shown here. Again, all experiments shown in Figure 10 were performed for the same dry diameter, i.e., 84 nm, at the second DMA. Error bars result from the AMS inherent uncertainties (*x* direction) and the achieved accuracy in adjusting the critical supersaturation (*y* direction). Here also, no difference is recognizable between compacted and noncompacted soot particles.

[31] The correlation between measured critical supersaturations and measured mass of coating was again better for ammonium (hydrogen) sulfate (+propanol) than for levoglucosan coating, with R^2 values of 0.87 and 0.56, respectively.

[32] From Figure 10 it can be seen, that for comparable masses of coating, particles coated with levoglucosan activated at higher supersaturations than particles coated with ammonium (hydrogen) sulfate (+propanol). This is consistent with the observations regarding the hygroscopic growth factors discussed above; that is, it is due to the lower hygro-

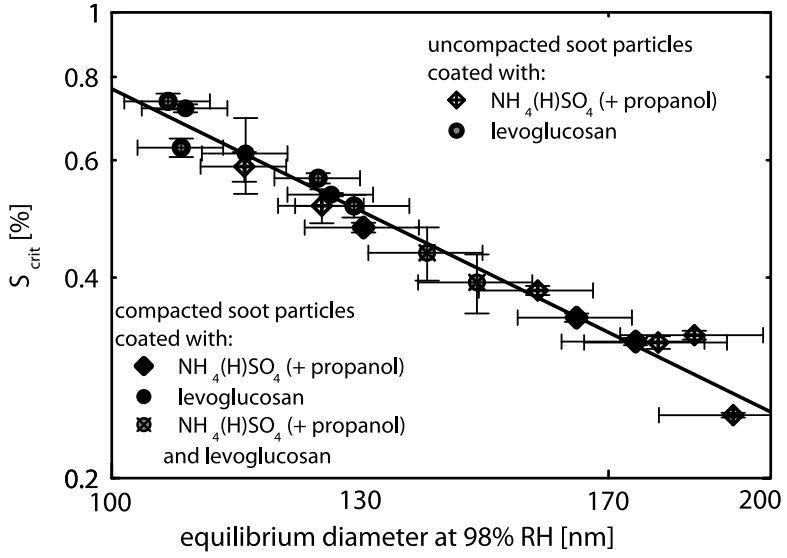

Figure 11. Comparison of the measured hygroscopic growth at a relative humidity of 98% and the measured critical supersaturations for the activation of different coated soot particles with a dry diameter of 84 nm.

scopicity of levoglucosan compared to that of the mixture of ammonium (hydrogen) sulfate and propanol.

8. Relation Between Particle Hygroscopic Growth and Activation Behavior

[33] Figure 11 shows the droplet equilibrium diameter at RH = 98% as function of critical supersaturation. Similar to Figures 9 and 10, error bars result from the achieved accuracy in adjusting relative humidity (*x* direction) and critical supersaturation (*y* direction). The correlation between hygroscopic growth and the critical supersaturation of the particles investigated indicates a clear relationship between these two properties. In addition data for soot particles coated with either ammonium (hydrogen) sulfate or levoglucosan, also data for soot particles that were coated with both, ammonium (hydrogen) sulfate and levoglucosan, are shown.

[34] As could be seen earlier in Figures 9 and 10, the droplet equilibrium diameter, which is proportional to the hygroscopic growth factor, increases and the critical supersaturation decreases with increasing coating mass. Hence, the critical supersaturation decreases with increasing hygroscopic growth. It also should be noted, that all the data for the differently coated soot particles fall onto the same line. The good correlation between hygroscopic growth and critical supersaturation (R^2 of 0.96 in the log-log illustration given in Figure 11), independent of the coating substance, suggests that predictions of critical supersaturations of coated soot particles should be possible based on measured hygroscopic growth data.

[35] The correlation found between measured hygroscopic growth and critical supersaturation is better than that found when correlating mass of the coating as determined from the AMS with either hygroscopic growth or activation. Both the hygroscopic growth and activation studies measure properties of the same Köhler curve but in the subsaturated and supersaturated regimes. This explains the good correlation between these measurements. The somewhat poorer correlation between hygroscopic growth, activation and the measured AMS masses can be explained by AMS inherent uncertainties.

[36] The topics of hygroscopic growth, activation and a more detailed study on how hygroscopic growth and activation properties can be related to each other, including Köhler-equation-based modeling of the behavior of the coated particles, will be described by *Henning et al.* [2010].

9. Summary and Conclusions

[37] During the LExNo campaign laboratory generated, two- and three-component particles consisting of soot, levoglucosan and ammonium (hydrogen) sulfate (+propanol) were investigated. The purpose was to mimic aged combustion aerosols, with respect to their composition and morphology, their hygroscopic properties, and their activation to droplets. A multimethodological approach was applied including chemical characterization, wherein the measurements of relevant particle properties were doubly covered. As a result of the coating procedure, the ammonium sulfate coating consisted of hydrogen sulfate and propanol. This was detected and quantified only because of the multimethodological approach which had foreseen control of the composition of the generated particles. The occurrence of propanol is an artifact that needs closer investigation and a modification of the coating procedure, but does not affect the results of the methodological comparison presented here. Since the coating composition was quantified it can be even considered in more detailed studies.

[38] Vacuum aerosol dynamic diameters D_{vae} were determined by low-pressure impactor LPI and aerosol mass spectrometers of Aerodyne Quadrupole AMS type. The agreement between the different instruments was found to be good for all different types of particles investigated in this study.

[39] The comparison of critical supersaturations for droplet activation measured with the three different CCN instruments and LACIS showed an excellent agreement within the measurement uncertainty, with systematically slightly larger values measured with LACIS. This is remarkable considering that the two types of CCN instruments and LACIS are based on different designs and operating principles. To our knowledge such a successful, comprehensive intercomparison of CCN instruments under controlled conditions was not reported in literature before.

[40] Hygroscopic growth measurements at relative humidities above 95% and CCN activation at supersaturations below 1% were tested for common trends. We found clear correlations between hygroscopic growth (equilibrium diameter at 98%) and activation behavior (critical supersaturation) for all investigated particle types. All three types of coated particles fall on the same single line. This suggests the validity of the same theory for both processes and allows for predicting the critical supersaturation of coated soot particles based on hygroscopic growth measurements. The actual prediction and the applied Köhler theory is presented in detail in the companion papers by *Henning et al.* [2010] and *Snider et al.* [2010].

[41] Relations were also found between the hygroscopic growth factor at 98% RH and the coating mass, as well as the critical supersaturation and coating mass as determined by the AMS. However, here the scattering around the regression line was stronger than in the hygroscopic growth–critical supersaturation relation. More detailed investigations on the LExNo data set are described in the companion papers: (1) the measurement of aerodynamic particle sizes using LPI and AMS [*Kiselev et al.*, 2010], (2) the comparability of the different CCN instruments used [*Snider et al.*, 2010], and (3) how hygroscopic growth and activation properties measured during LExNo can be related to each other and to soluble mass determined by AMS [*Henning et al.*, 2010].

[42] By the results of the multiple instrumental comparisons within the LExNo campaign presented here, we intended to further establish the Leipzig Aerosol Cloud Interaction Simulator (LACIS) and its related infrastructure as a powerful scientific tool to study hygroscopic growth and activation to cloud droplets of complex, multicomponent particles. The comparison of the LACIS periphery and the LACIS instrument itself with AMS, HH-TDMA and two types of CCN instruments revealed the high accuracy of LACIS as well as the ability to run controlled and reproducible simulation experiments. Please note, that with LACIS

subsaturated and supersaturated regime of particle growth can be achieved within the same instrumental setup.

[43] **Acknowledgments.** LExNo collaborators whose travel to Leipzig and whose accommodations in Leipzig were supported by ACCENT acknowledge that financial support and wish to thank ACCENT for making their involvement in LExNo a reality. These participants were, in alphabetical order, U. Dusek, G. Frank, A. Kiendler-Scharr, A. Kristensson, T. F. Mentel, D. Rose, J. Snider, and S. Walter. M. Bilde and A. Kristensson acknowledge BACCI and FORMAS for support.

References

Alfarra, M. R., A. S. H. Prévôt, S. Szidat, J. Sandradewi, S. Weimer, V. A. Lanz, D. Schreiber, M. Mohr, and U. Baltensperger (2007), Identification of the mass spectral signature of organic aerosols from wood burning emissions, *Environ. Sci. Technol.*, *41*, 5770–5777, doi:10.1021/es062289b.

Allan, J. D., et al. (2004), Technical note: Extraction of chemically resolved mass spectra from aerodyne aerosol mass spectrometer data, *J. Aerosol Sci.*, *35*, 909–922, doi:10.1016/j.jaerosci.2004.02.007.

Andreae, M. O., and P. Merlet (2001), Emissions of trace gases and aerosols from biomass burning, *Global Biogeochem. Cycles*, *15*, 955–966, doi:10.1029/2000GB001382.

Bilde, M., and B. Svenningsson (2004), CCN activation of slightly soluble organics: Importance of small amounts of inorganic salt and particle phase, *Tellus, Ser. B*, *56*, 128–134.

Broekhuizen, K., R. Y.-W. Chang, W. R. Leaitch, S.-M. Li, and J. P. D. Abbatt (2006), Closure between measured and modeled cloud condensation nuclei (CCN) using size-resolved aerosol composition in downtown Toronto, *Atmos. Chem. Phys.*, *6*, 2513–2524.

Fernández de la Mora, J. F., N. Rao, and P. McMurry (1990), Inertial impaction of fine particles at moderate Reynolds numbers and in the transonic regime with a thin-plate orifice, *J. Aerosol Sci.*, *21*, 889–909, doi:10.1016/0021-8502(90)90160-Y.

Forster, P., et al. (2007), Changes in atmospheric constituents and in radiative forcing, in *Climate Change 2007: The Physical Science Basis. Contribution of Working Group I to the Fourth Assessment Report of the Intergovernmental Panel on Climate Change*, pp. 131–234, Cambridge Univ. Press, New York.

Graham, B., O. L. Mayol-Bracero, P. Guyon, G. C. Roberts, S. Decesari, M. C. Facchini, P. Artaxo, W. Maenhaut, P. Köll, and M. O. Andreae (2002), Water-soluble organic compounds in biomass burning aerosols over Amazonia: 1. Characterization by NMR and GC-MS, *J. Geophys. Res.*, *107*(D20), 8047, doi:10.1029/2001JD000336.

Halstead, D. W. (1970), Thermal decomposition of ammonium-sulfate, *J. Appl. Chem. USSR*, *20*(4), 129–132.

Hennig, T., A. Massling, F. Brechtel, and A. Wiedensohler (2005), A tandem DMA for highly temperature-stabilized hygroscopic particle growth measurements between 90% and 98% relative humidity, *J. Aerosol Sci.*, *36*, 1210–1223, doi:10.1016/j.jaerosci.2005.01.005.

Henning, S., et al. (2010), Soluble mass, hygroscopic growth, and droplet activation of coated soot particles during LACIS Experiment in November (LExNo), *J. Geophys. Res.*, *115*, D11206, doi:10.1029/2009JD012626.

Jayne, J. T., D. C. Leard, X. Zhang, P. Davidovits, K. A. Smith, C. E. Kolb, and D. R. Worsnop (2000), Development of an aerosol mass spectrometer for size and composition analysis of submicron particles, *Aerosol Sci. Technol.*, *33*, 49–70, doi:10.1080/027868200410840.

Kawamoto, H., W. Hatanaka, and S. Saka (2003), Thermochemical conversion of cellulose in polar solvent (sulfolane) into levoglucosan and other low molecular-weight substances, *J. Anal. Appl. Pyrolysis*, *70*(2), 303–313, doi:10.1016/S0165-2370(02)00160-2.

Kiselev, A., C. Wennrich, F. Stratmann, H. Wex, S. Henning, T. F. Mentel, A. Kiendler-Scharr, J. Schneider, S. Walter, and I. Lieberwirth (2010), Morphological characterization of soot aerosol particles during LACIS Experiment in November (LExNo), *J. Geophys. Res.*, *115*, D11204, doi:10.1029/2009JD012635.

Kiyoura, R., and K. Urano (1970), Mechanism, kinetics, and equilibrium of thermal decomposition of ammonium-sulfate, *Ind. Eng. Chem. Process Des. Dev.*, *9*(4), 489–494, doi:10.1021/i260036a001.

Kütz, S. (1994), In-situ Methoden zur Bestimmung von Struktureigenschaften gasgetragener Agglomerate, Ph.D. thesis, Univ. of Duisburg, Duisburg, Germany.

Lance, S., J. Medina, J. N. Smith, and A. Nenes (2006), Mapping the operation of the DMT continuous flow CCN counter, *Aerosol Sci. Technol.*, *40*, 242–254, doi:10.1080/02786820500543290.

Medina, J., A. Nenes, R.-E. P. Sotiropoulou, L. D. Cottrell, L. D. Ziemba, P. J. Beckman, and R. J. Griffin (2007), Cloud condensation nuclei closure during the International Consortium for Atmospheric Research on Transport and Transformation 2004 campaign: Effects of size-resolved composition, *J. Geophys. Res.*, *112*, D10S31, doi:10.1029/2006JD007588.

Messerer, A., R. Niessner, and U. Poeschl (2003), Thermophoretic deposition of soot aerosol particles und experimental conditions relevant for modern diesel engine exhaust gas systems, *J. Aerosol Sci.*, *34*, 1009–1021, doi:10.1016/S0021-8502(03)00081-8.

Mochida, M., and K. Kawamura (2004), Hygroscopic properties of levoglucosan and related organic compounds characteristic to biomass burning aerosol particles, *J. Geophys. Res.*, *109*, D21202, doi:10.1029/2004JD004962.

Oja, V., and E. M. Suuberg (1999), Vapor pressures and enthalpies of sublimation of D-glucose, d-xylose, cellobiose, and levoglucosan, *J. Chem. Eng. Data*, *44*, 26–29, doi:10.1021/je980119b.

Reid, J. S., R. Koppmann, T. F. Eck, and D. P. Eleuterio (2005a), A review of biomass burning emissions part II: Intensive physical properties of biomass burning particles, *Atmos. Chem. Phys.*, *5*, 799–825.

Reid, J. S., T. F. Eck, S. A. Christopher, R. Koppmann, O. Dubovik, D. P. Eleuterio, B. N. Holben, E. A. Reid, and J. Zhang (2005b), A review of biomass burning emissions part III: Intensive optical properties of biomass burning particles, *Atmos. Chem. Phys.*, *5*, 827–849.

Roberts, G., and A. Nenes (2005), A continuous-flow streamwise thermal-gradient CCN chamber for atmospheric measurements, *Aerosol Sci. Technol.*, *39*, 206–221, doi:10.1080/027868290913988.

Rose, D., S. S. Gunthe, E. Mikhailov, G. P. Frank, U. Dusek, M. O. Andreae, and U. Pöschl (2008), Calibration and measurement uncertainties of a continuous-flow cloud condensation nuclei counter (DMT-CCNC): CCN activation of ammonium-sulfate and sodium chloride aerosol particles in theory and experiment, *Atmos. Chem. Phys.*, *8*, 1153–1179.

Schneider, J., S. Weimer, F. Drewnick, S. Borrmann, G. Helas, P. Gwaze, O. Schmid, M. O. Andreae, and U. Kirchner (2006), Mass spectrometric analysis and aerodynamic properties of various types of combustion-related aerosol particles, *Int. J. Mass Spectrom.*, *258*(1–3), 37–49, doi:10.1016/j.ijms.2006.07.008.

Seinfeld, J. H., and S. N. Pandis (1998), *Atmospheric Chemistry and Physics*, 1326 pp., John Wiley, Hoboken, N. J.

Simoneit, B. R. T., J. J. Schauer, C. G. Nolte, D. R. Oros, V. O. Elias, M. P. Fraser, W. F. Rogge, and G. R. Cass (1999), Levoglucosan, a tracer for cellulose in biomass burning and atmospheric particles, *Atmos. Environ.*, *33*, 173–182, doi:10.1016/S1352-2310(98)00145-9.

Simpson, C. D., R. L. Dills, B. S. Katz, and D. A. Kalman (2004), Determination of levoglucosan in atmospheric fine particulate matter, *J. Air Waste Manage. Assoc.*, *54*, 689–694.

Snider, J. R., S. Guibert, J.-L. Brenguier, and J. P. Putaud (2003), Aerosol activation in marine stratocumulus clouds: 2. Köhler and parcel theory closure studies, *J. Geophys. Res.*, *108*(D15), 8629, doi:10.1029/2002JD002692.

Snider, J. R., M. D. Petters, P. Wechsler, and P. S. K. Liu (2006), Supersaturation in the Wyoming CCN instrument, *J. Atmos. Oceanic Technol.*, *23*, 1323–1339, doi:10.1175/JTECH1916.1.

Snider, J. R., et al. (2010), Intercomparison of cloud condensation nuclei and hygroscopic fraction measurements: Coated soot particles investigated during the LACIS Experiment in November (LExNo), *J. Geophys. Res.*, *115*, D11205, doi:10.1029/2009JD012618.

Stratmann, F., A. Kiselev, S. Wurzler, M. Wendisch, J. Heintzenberg, R. J. Charlson, K. Diehl, H. Wex, and S. Schmidt (2004), Laboratory studies and numerical simulations of cloud droplet formation under realistic supersaturation conditions, *J. Atmos. Oceanic Technol.*, *21*, 876–887, doi:10.1175/1520-0426(2004)021<0876:LSANSO>2.0.CO;2.

Stroud, C. A., et al. (2007), Cloud activating properties of aerosol observed during CELTIC, *J. Atmos. Sci.*, *64*, 441–459, doi:10.1175/JAS3843.1.

Van Gulijk, C., J. C. M. Marijnissen, M. Makkee, J. A. Moulijn, and A. Schmidt-Ott (2004), Measuring diesel soot with a scanning mobility particle sizer and an electrical low-pressure impactor: Performance assessment with a model for fractal-like agglomerates, *J. Aerosol Sci.*, *35*, 633–655, doi:10.1016/j.jaerosci.2003.11.004.

Wex, H., A. Kiselev, F. Stratmann, J. Zoboki, and F. Brechtel (2005), Measured and modeled equilibrium sizes of NaCl and (NH4)2SO4 particles at relative humidities up to 99.1%, *J. Geophys. Res.*, *110*, D21212, doi:10.1029/2004JD005507.

Wex, H., A. Kiselev, M. Ziese, and F. Stratmann (2006), Calibration of LACIS as a CCN detector and its use in measuring activation and hygroscopic growth of atmospheric aerosol particles, *Atmos. Chem. Phys.*, *6*, 4519–4527.

Wex, H., F. Stratmann, T. Hennig, S. Hartmann, D. Niedermeier, E. Nilsson, R. Ocskay, D. Rose, I. Salma, and M. Ziese (2008), Connecting hygro-

scopic growth at high humidities to cloud activation for different particle types, *Environ. Res. Lett.*, *3*, 035004, doi:10.1088/1748-9326/1083/1082/035004.

Winklmayr, W., et al. (1991), A new electromobility spectrometer for the measurement of aerosol size distributions in the size range from 1 to 1000 nm, *J. Aerosol Sci.*, *22*, 289–296, doi:10.1016/S0021-8502(05)80007-2.

Zdrahal, Z., J. Oliveira, R. Vermeylen, M. Claeys, and W. Maenhaut (2002), Improved method for quantifying levoglucosan and related monosaccharide anhydrides in atmospheric aerosols ad application to samples from urban and tropical locations, *Environ. Sci. Technol.*, *36*, 747–753, doi:10.1021/es015619v.

M. Bilde, Department of Chemistry, University of Copenhagen, Universitetsparken 5, DK-2100 Copenhagen, Denmark.

U. Dusek, Institute for Marine and Atmospheric Research, Utrecht University, Princetonplein 5, NL-3584 CC Utrecht, Netherlands.

G. P. Frank and A. Kristensson, Department of Physics, Lund University, Box 118, SE-22100 Lund, Sweden.

T. Hennig, Institute for Applied Environmental Science, Stockholm University, Svante Arrhenius väg 8, SE-10691 Stockholm, Sweden.

S. Henning, A. Kiselev, F. Stratmann, and H. Wex, Institute for Tropospheric Research, Department of Physics, Permoser Str. 15, D-04318, Leipzig, Germany. (straddi@tropos.de)

A. Kiendler-Scharr, T. F. Mentel, and R. Tillmann, ICG-II: Troposphere, Juelich Research Centre, D-52425 Juelich, Germany.

I. Lieberwirth, Max Planck Institute for Polymer Research, D-55128 Mainz, Germany.

U. Pöschl and D. Rose, Biogeochemistry Department, Max Planck Institute for Chemistry, PO Box 3060, D-55020 Mainz, Germany.

J. Schneider and S. Walter, Particle Chemistry Department, Max Planck Institute for Chemistry, Joh.-Joachim-Becher Weg 27, D-55128 Mainz, Germany.

J. R. Snider, Department of Atmospheric Science, University of Wyoming, Dep. 3038, 1000 E. University Ave., Laramie, WY 82071, USA.